

Aromatic Polymer with Pendant Perfluoroalkyl Sulfonic Acid for Fuel Cell Applications

Ken Yoshimura* and Katsuhiko Iwasaki

Tsukuba Research Laboratory, Sumitomo Chemical Co., Ltd., 6 Kitahara, Tsukuba, Ibaraki, 300-3294 Japan

Received September 2, 2009; Revised Manuscript Received October 7, 2009

ABSTRACT: Novel proton exchange membranes were prepared and investigated as polymer electrolyte membranes (PEMs) for polymer electrolyte membrane fuel cells (PEMFCs). Polymers having poly(arylene ether sulfone) in the main chain and $-\text{CF}_2\text{CF}_2\text{OCF}_2\text{CF}_2\text{SO}_3\text{H}$ in the side chain (PES-PSA) were synthesized by dehalogen coupling of poly{oxy-4,4'-(3,3'-dibromobiphenylene)oxy-4,4'-diphenylsulfone} (PES-Br) and potassium 1,1,2,2-tetrafluoro-2-(1,1,2,2-tetrafluoro-2-iodoethoxy)ethanesulfonate (PSA-K) using copper metal, followed by treatment with aqueous HCl. The proton conductivity of PES-PSA with an ion exchange capacity (IEC) of 1.58 mmol/g was 0.12 S/cm at 80 °C under 90% relative humidity. PES-PSA with an IEC of 1.34 mmol/g was used as the membrane for PEMFC, and the maximum power output at 80 °C was 805 mW/cm² when fully humidified hydrogen and air were provided. A DMA measurement and a tensile test revealed that PES-PSA had a higher α -relaxation temperature than Nafion and higher flexibility than sulfonated polyethersulfone (SPES).

1. Introduction

The polymer electrolyte membrane fuel cell (PEMFC) has attracted much attention as a future source of clean energy. In the PEMFC, electric power is generated when an oxonium ion and oxygen react on the cathode. To react efficiently, the oxonium ion must migrate with little resistance through a polymer electrolyte membrane (PEM). The most-used proton-conducting polymers are sulfonated perfluoropolymers such as Nafion (DuPont) because of their high proton conductivity and high chemical stability. It is considered that high conductivity is caused by perfluoroalkyl sulfonic acid acting as a super acid. However, the practical use of such polymers suffers from high cost and low α -relaxation temperature at ~ 100 °C.¹ The low α -relaxation temperature is due to the aliphatic structure in the main chain and causes a low operation temperature in the fuel cell. To obtain high energy efficiency and avoid poisoning the Pt catalyst with carbon monoxide, a higher operation temperature is required.

Recently, the development of inexpensive and heat-resistant electrolyte membranes that can be substituted for the perfluorinated membranes has attracted our attention. Among others, polymer electrolyte membranes obtained by introducing a sulfonic acid group into an aromatic polymer demonstrate excellent heat resistance.^{2–18} Improved durability and mobility of the sulfonic acid group were reported in polymers having aromatic rings in the main chain and alkyl sulfonic acid in the side chain.^{19–21} Also, it has been suggested that stronger acids tend to be better proton conductors because they can be deprotonated easily under less humid conditions.²²

We focused on polymer electrolytes having aromatic rings in the main chain and perfluoroalkyl sulfonic acid in the side chain, which were expected to exhibit high thermal stability and high proton conductivity because of the aromatic rings and perfluoroalkyl sulfonic acid, respectively. In this report, we investigate the first synthesis of this novel class of polymer electrolyte having

aromatic rings in the main chain and perfluoroalkyl sulfonic acid as the branch. We also discuss their proton conductivity, morphology, thermoviscoelastic behavior, mechanical strength, and fuel cell performance.

2. Experimental Section

2.1. Materials and Measurements. 1,1,2,2-Tetrafluoro-2-(1,1,2,2-tetrafluoro-2-iodoethoxy)ethanesulfonyl fluoride (PSA-F) was purchased from SynQuest Laboratories and was used as received. 2,6-Lutidine and 1 M solution of tetra-*n*-butylammonium fluoride in tetrahydrofuran (THF) were purchased from Tokyo Kasei Kogyo and dried over molecular sieves prior to use. Poly(oxy-4,4'-biphenyleneoxy-4,4'-diphenylsulfone) (PPSf), Nafion112, and Nafion 5% solution were purchased from Sigma-Aldrich and were used as received. Dimethylsulfoxide (DMSO), *N,N*-dimethylacetamide (DMAc), toluene, and methylene chloride were purchased from Wako Pure Chemical Industries and dried over molecular sieves prior to use. All other chemicals were reagent grade and were used as received. ¹H NMR and ¹⁹F NMR spectra were recorded on a Varian INOVA 300 instrument at 299.404 and 281.699 MHz, respectively.

2.2. Synthesis of Potassium 1,1,2,2-Tetrafluoro-2-(1,1,2,2-tetrafluoro-2-iodoethoxy) Ethanesulfonate (2) (PSA-K). To a solution of PSA-F (15.0 g, 35.2 mmol) in dichloromethane (5 mL) were added water (5.0 mL), 2,6-lutidine (4.80 g, 44.8 mmol), and a 1 M solution of tetra-*n*-butylammonium fluoride in THF (0.1 mL). The reaction mixture was stirred vigorously at room temperature for 4 days and was extracted with dichloromethane (50 mL \times 3), and the solvent was removed under reduced pressure. The residue was diluted with THF (10 mL), and potassium carbonate (2.82 g, 20.4 mmol) was added, followed by stirring at room temperature for 10 h. The remaining solid was filtered off, and the filtrate was concentrated to yield a solid. The solid was recrystallized from a mixture of THF/toluene (1/1) to obtain 12.3 g (82.4%) of potassium 1,1,2,2-tetrafluoro-2-(1,1,2,2-tetrafluoro-2-iodoethoxy) ethanesulfonate (2) (PSA-K) as a white solid. ¹⁹F NMR spectrum in DMSO-*d*₆ (ppm) (Figure 1, bottom): -74.85 , -84.55 , -88.11 ,

*Corresponding author. E-mail: yoshimurak2@sc.sumitomo-chem.co.jp. Tel: +81-29-864-4172. Fax: +81-29-864-4747.

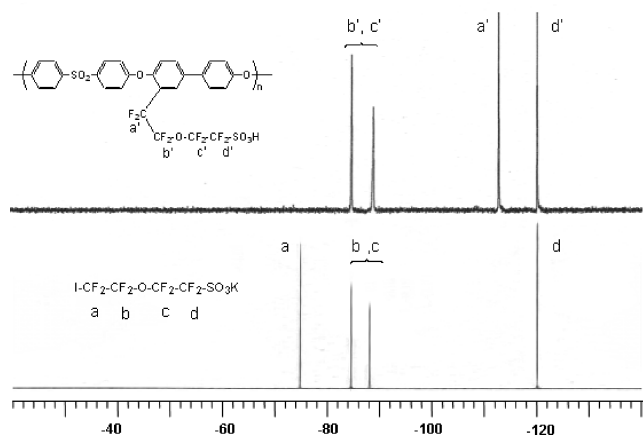


Figure 1. ^{19}F NMR spectra of PSA-K (**2**) (bottom) and PES-PSA (**3**) (top) in $\text{DMSO}-d_6$.

−120.17. Elemental analysis: Calculated: F, 32.9 wt %. Found: F, 33.1 wt %.

2.3. Typical Synthesis Procedure for a Polymer Having Pendant Perfluoro-Oxyalkyl Sulfonic Acid (PES-PSA) (3**) (A7 in Table 1).** To a solution of poly{oxy-4,4'-(3,3'-dibromobiphenylene)oxy-4,4'-diphenylsulfone} (PES-Br, **1**; see Supporting Information for preparation) (2.00 g) in DMSO (10 mL) was added copper powder (<200 mesh) (1.97 g, 31.9 mmol) under nitrogen, and the reaction mixture was stirred at 120 °C for 2 h. To the reaction mixture was added PSA-K (**2**) 4.00 g (8.66 mmol) in 10 mL of DMSO, and the reaction mixture was stirred for 6 h at 120 °C. The reaction mixture was allowed to decrease to room temperature and was filtered using Celite, and the filtrate was added to a 5 N HCl solution to precipitate crude PES-PSA (**3**) (acid form). The crude PES-PSA was thoroughly washed with 5 N aqueous HCl, washed with water, and dried to obtain 2.52 g of PES-PSA (**3**). ^{19}F NMR spectrum in $\text{DMSO}-d_6$ (ppm) (Figure 1, top): −84.62, −88.81, −112.92, −120.28. Elemental analysis: Found: Br, 0.2 wt %.

2.4. Preparation of Membrane and Characterization. The resulting polymers were dissolved in DMAc at room temperature, and the solution was filtered using a Teflon filter (pore size: 0.45 μm). The filtrate was spread onto a glass plate and placed in an oven at 80 °C to remove the solvent. The membranes were peeled off from the glass plate, and to convert the remaining salt form to acid form, we rinsed the membranes in 2 N HCl for 2 h and then washed with deionized water. The membranes were dried and stored in hermetic plastic bags. Adjusting the concentration of the solution controlled the thickness of the resulting membrane.

Proton conductivity parallel to the surface (in-plane) of the membrane was determined by alternating-current impedance spectroscopy using a potentiostat-galvanostat impedance analyzer system 12608W (TOYO Corporation) in a range of 100 kHz to 0.01 Hz. The impedance measurements were performed at 80 °C under 50, 70, and 90% relative humidity (RH). Through-plane proton conductivity was determined by the following modified method described elsewhere.²³ A membrane that was swollen in a 1 mol/L sulfuric acid solution was placed between two carbon electrodes (1 cm^2) with silicon rubber having an opening of 1 cm^2 as a gasket, and the resulting cell was immersed in 1 mol/L of sulfuric acid; then, the value of resistance was measured by the alternating-current impedance method at 23 °C by subtracting the background impedance of 1 mol/L of sulfuric acid. The measurement of the through-plane conductivity was conducted three times on each sample and was determined by averaging them.

The ion exchange capacity (IEC) was determined by acid–base back-titration using 0.1 N HCl and 0.1 N NaOH. Water uptake by the membrane was determined by the weight difference of the

weight between dry and hydrated membranes. The wet membrane was prepared by soaking in 80 °C water for 2 h. The water uptake was determined by the following equation

$$\text{water uptake (wt \%)} = 100 \times (W_{\text{wet}} - W_{\text{dry}}) / W_{\text{dry}}$$

where W_{wet} is the membrane weight of wet state and W_{dry} is the membrane weight of dry state.

Dynamic mechanical analysis (DMA) was performed with a DMA 2980 (TA Instruments) at 10 Hz with a ramp rate of 2 °C/min.

A tensile test was performed by Autograph AGS-X (Shimadzu) with a crosshead speed of 5 mm/min at 23 °C using a test piece prepared by the Super Dumbbell Cutter SDK-300. The elastic module and the breaking elongation of the membranes were measured using five test pieces, of which the minimum and maximum values were omitted, and the remaining three data were averaged. The wet membrane was prepared by immersion in deionized water at 23 °C for 24 h, and the water adhering to the surface was wiped off just before use.

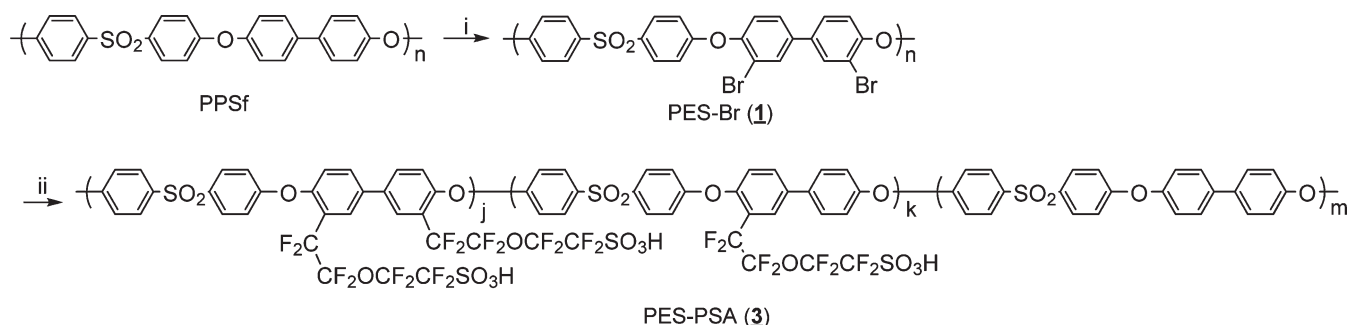
Synchrotron SAXS experiments were performed at BL-15A in the High-Energy Accelerator Research Organization (KEK), Japan. The X-ray wavelength and the sample-to-detector distance were 0.1504 nm and 2250 mm, respectively. The sample was sealed by the thin film of the Vectra A950 to maintain the water content of the membrane and was measured using blank Vectra as the background. An imaging plate was used as the detector to explore the q values, where q is the scattering vector ($q = (4\pi \sin \theta) / \lambda$) and 2θ is the total scattering angle.

A fuel cell performance was performed as follows. A Nafion 5% solution purchased from Aldrich was added to Pt on carbon (30% Pt), to which isopropanol was added. The mixture was coated on a carbon cloth (E-TEK Vulcan XC-72) and dried to obtain electrodes containing 0.6 mg/cm^2 of Pt. A membrane of PES-PSA or Nafion112 was sandwiched between the two 5 cm^2 electrodes and was placed in a fuel cell with a 5 cm^2 gas flow area purchased from Electrochem. Hydrogen and air were humidified by flowing through a bubbler at 80 °C and were fed into the fuel cell. The fuel cell performance measurements were carried out at 80 °C using an electronic load and electrometer.

3. Results and Discussion

3.1. Synthesis of the PES-PSA. Scheme 1 shows the synthesis route of PES-PSA. Potassium 1,1,2,2-tetrafluoro-2-(1,1,2,2-tetrafluoro-2-iodoethoxy) ethanesulfonate (**2**) (PSA-K) was prepared by the hydrolysis of commercially available 1,1,2,2-tetrafluoro-2-(1,1,2,2-tetrafluoro-2-iodoethoxy)ethanesulfonyl fluoride in the presence of both 2, 6-lutidine as a base and tetra-*n*-butylammonium fluoride as a phase-transfer catalyst at room temperature, followed by neutralization using potassium carbonate (Figure 1, bottom). Initial attempts to cross-couple the PSA-K and polymer were unsuccessful. Williamson ether synthesis using a polymer having a hydroxyl group {poly(−C₆H₄−SO₂−C₆H₄−O−C₆H₃(OH)−)} and PSA-K using potassium carbonate, a nucleophilic reaction using lithio-polysulfone {poly(−C₆H₃Li−SO₂−C₆H₄−O−C₆H₄−C(CH₃)₂−C₆H₄−O−)} and PSA-K, as well as a Friedel–Crafts reaction using PPSf and PSA-K in the presence of AlCl₃ did not proceed or gave only some undesired byproduct.

The introduction of a perfluoroalkyl unit to an aromatic ring has been demonstrated by the reaction of perfluorohalide with an aromatic halide using copper metal.^{25–27} This synthetic reaction procedure was incorporated into the reaction of PES-Br and PSA-K. The PES-Br was easily prepared by bromination of PPSf using bromine at room temperature,²⁴ and according to ^1H NMR and elemental analysis of PES-Br, approximately two bromine atoms

Scheme 1. Synthetic Route of PES-PSA (3)^a

^a (i) Br₂, CH₂Cl₂, 0 °C to r.t., 4 h. (ii) (1) Cu, DMSO, 120 °C, 2 h; (2) PSA-K(2), DMSO, 120 °C, 2 h; (3) HCl, r.t.

Table 1. Proton Conductivity, Water Uptake, and IEC Data of PES-PSAs and SPESs

entry	type	proton conductivity at 80 °C (S/cm)			water uptake wt %	IEC ^a meq/g
		90% RH	70% RH	50% RH		
A1	PES-PSA	0.015	0.0032	0.00033	20	0.95
A2		0.028	0.0071	0.0010	28	1.05
A3		0.038	0.012	0.0029	51	1.16
A4		0.049	0.013	0.0023	65	1.25
A5		0.077	0.024	0.0055	92	1.34
A6		0.089	0.024	0.0056	132	1.48
A7		0.12	0.032	0.0089	185	1.58
B1	SPES	0.0078	0.0021	0.00021	47	1.08
B2		0.021	0.0073	0.00078	88	1.33
B3		0.035	0.013	0.0016	172	1.51

^a Ion exchange capacity.

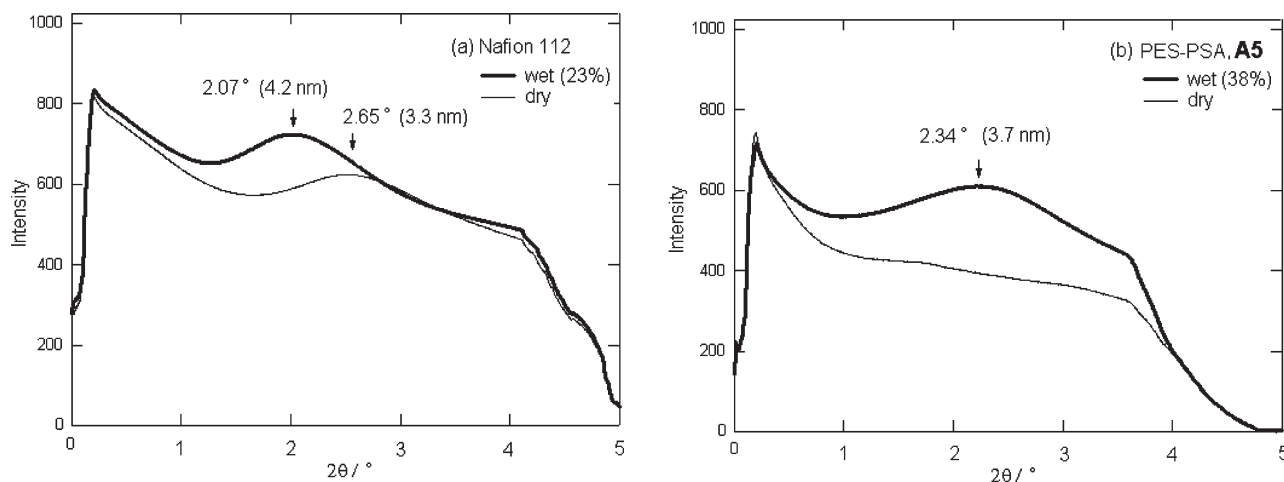


Figure 2. SAXS profiles of (a) Nafion 112 and (b) PES-PSA (A5).

were introduced per one repeating unit. During the coupling reaction, a peak at -74.85 ppm in the ^{19}F NMR, which was assigned to the fluorine group of $\text{I}-\text{CF}_2-$, decreased in intensity, and a new peak at -112.92 ppm, which was assigned to the fluorine group of $\text{Ar}-\text{CF}_2-$ (Ar: aromatic ring), emerged and increased in intensity (Figure 1, top). Anhydrous PES-Br, PSA-K, and DMSO should be used because the coupling reaction was sensitive to moisture. In the presence of moisture, the introduction rate of the PSA-K could not be controlled. No gelation was observed, which meant the coupling reaction between polymer chains did not take place under this condition. From the elemental analysis of PES-PSA, almost no bromine was detected, which indicated that activated bromine during reaction was protonated by quenching process.

3.2. Characteristics of PES-PSA. The results of the characterization of PES-PSA and sulfonated polysulfone (SPES,

see the Supporting Information for preparation) were summarized in Table 1. The proton conductivities of PES-PSAs were higher than those of SPESs at any IEC level and under any humid condition, although the IEC dependence on the water uptake behavior of PES-PSA was similar to that of SPES. One should consider the possibility that the acidity of the perfluoroalkyl sulfonic acid of PES-PSA is significantly high compared with that of the aromatic sulfonic acid of the SPES, which caused easy sulfonic acid dissociation and showed higher proton conductivity.

PES-PSA, having IEC of > 1.4 meq/g, absorbed water of 100 wt % and up. This distinctive behavior is thought to be related to the microphase separation in the membrane.²⁸ It is reported that there are ion-cluster channels in Nafion, which contribute to proton conduction and retention of membrane shape.²⁹ To investigate the state of the ion-cluster channel of PES-PSA, SAXS experiments were performed (Figure 2).

The size of the cluster channel of dry Nafion was found to be 3.3 nm, however, no significant peak was observed for dry PES-PSA. After water was absorbed in the PES-PSA, the cluster channel formed, and the size of the cluster channel of the wet PES-PSA (water content = 38 wt %) was 3.7 nm. The cluster channel of the wet PES-PSA was smaller than that of Nafion (4.2 nm, water content = 23 wt %), even though the water content of PES-PSA was higher than that of Nafion. These phenomena indicate that less aggregation of the side chain occurred in the PES-PSA despite having similar side chains. This is probably due to the rigid main chain of the PES-PSA, which prevented aggregation of the side chain. It is likely that the difference in these microphase separations caused different IEC dependence on water uptake and proton conductivity. To enhance forming the ion cluster channel of PES-PSA, it would be effective to create a block copolymer comprising a hydrophilic unit having perfluoroalkyl sulfonic acid groups as the side chain and a hydrophobic unit not having proton-dissociating groups.⁶

3.3. Tensile Test. The results of the tensile test are summarized in Table 2. The breaking elongation of the PES-PSA, conditioned by placing membrane at 23 °C under 50% RH for 24 h (water content, $W_c = 6\%$), was higher than that of SPES ($W_c = 9\%$), which means the PES-PSA is more flexible than SPES in the dry state. This flexibility is an advantage for the start-and-stop operation of a fuel cell. The elastic module of the wet PES-PSA ($W_c = 45\%$) was higher than that of wet SPES ($W_c = 48\%$). The membrane in the fuel cell is always pressed by the bipolar plates; therefore, the higher elastic module of the PES-PSA in the wet state is important to avoid creep of the membrane. This elastic module and flexibility of the PES-PSA should have better durability under fuel cell operation.

Table 2. Tensile Test of PES-PSA and SPES^{a,b}

type	membrane state	water content (%) ^c	elastic module (MPa)	breaking elongation (%)
PES-PSA, A6	dry	9	793	119
	wet	45	112	143
SPES, B3	dry	6	823	44
	wet	48	76	84

^a Elastic modules and a breaking elongation of the membranes were measured using five test pieces, of which the minimum and maximum values were omitted and the remaining three data were averaged. ^b Dry membranes were prepared by placing at 23 °C for 24 h under 50% RH. Wet membranes were prepared by immersion in deionized water at 23 °C for 24 h and were wiped water of adhesion on the surface just before use. ^c Water content (W_c) was determined by the following equation: W_c (wt %) = $100 \times (W_{\text{sam}} - W_{\text{dry}}) / W_{\text{dry}}$ (herein, W_{sam} : weight of sample; W_{dry} : weight of dry membrane).

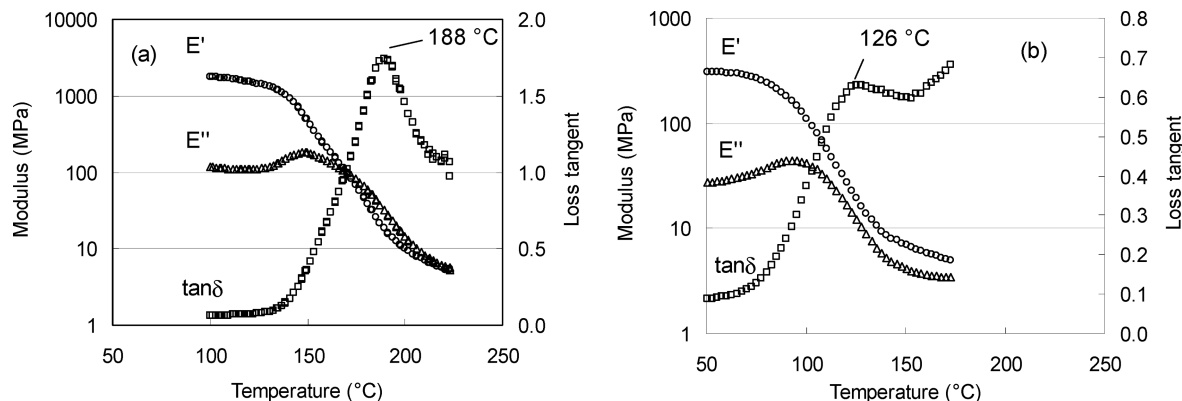


Figure 3. DMA traces of (a) PES-PSA (A5) and (b) Nafion112. Storage modulus (E' , \circ), loss modulus (E'' , Δ), and loss tangent ($\tan \delta$, \square).

3.4. Dynamic Mechanical Analysis. It is reported that β - and α -relaxation of Nafion were observed at -20 to 20 °C^{1,34} and 100 – 120 °C,^{1,31} respectively. In the temperature range between β - and α -relaxation, motions within the framework of a physically static cross-linked network were found, which meant that the hydrophilic and hydrophobic domains are morphologically fixed. At temperatures above α -relaxation, molecular mobility became considerable because of the loss of the hydrogen-bonding network, which indicated the disappearance of the microphase separation.^{1,30} From the standpoint of the practical use of the under fuel cell operation, the importance of the α -relaxation of the membrane is significant, because the α -relaxation in Nafion is related to the onset of the thermally activated motions of both the side chain and the main chain, giving rise to the gradual collapse of the static network and the subsequent evolution of a dynamic network.^{1,30,32,33}

To investigate the α -relaxation, we performed DMA on PES-PSA (A5) and Nafion112, as shown in Figure 3. In the DMA measurement, the α -relaxation temperature is nearly equal to the temperature at the maximum loss tangent ($\tan \delta = E'/E''$, wherein E' is the storage modulus and E'' is the loss modulus). The temperature at the maximum loss tangent of PES-PSA (188 °C) was higher than that of Nafion (126 °C), which confirmed that PES-PSA had a higher α -relaxation temperature than Nafion.

3.5. Fuel Cell Operation. Fuel cell performances using PES-PSA (A5, 47 μm) and Nafion112 (51 μm) were investigated. Although the in-plain proton conductivity of A5 (0.077 S/cm at 80 °C under 90%RH) is lower than that of

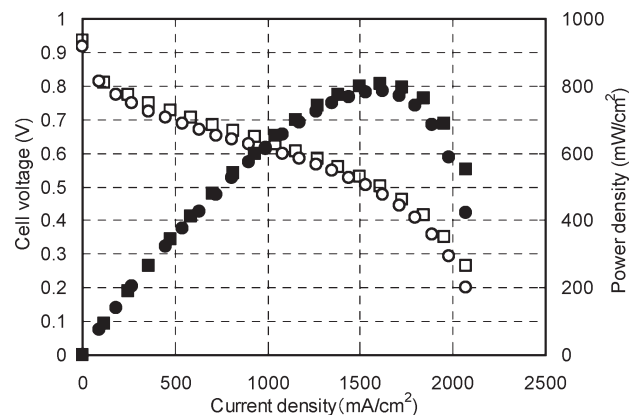


Figure 4. Polarization curves of PES-PSA (A5, 43 μm ; cell voltage: \square , power output: \blacksquare) and Nafion112 (51 μm ; cell voltage: \circ , power output: \bullet); Conditions: cell temperature = 80 °C; H_2/air ; 1.01×10^5 Pa; bubbler temperature = 80 °C; electrode area = 5 cm^2 .

Nafion (0.089 S/cm), the maximum power output of the PES-PSA was at the same level in comparison with Nafion (Figure 4). The through-plain proton conductivities²³ of Nafion and PES-PSA, which are practically important for fuel cell operation, were 0.060 and 0.063 S/cm, respectively. It makes no sense to compare the difference between in-plain and through-plain proton conductivity because of the condition difference of the measurement; however, it seems that the proton conduction anisotropy of PES-PSA is more favorable than that of Nafion. The difference in the proton conduction anisotropy between PES-PSA and Nafion is probably one of the reasons for the results of the fuel cell operation. As mentioned above, the microphase separation of PES-PSA was ambiguous compared with Nafion; therefore, a forming block copolymer comprising hydrophilic and hydrophobic segments would enhance the microphase separation, which should achieve better properties for fuel cell operation as well as water uptake.⁶ Further investigations, including chemical stability and long-term fuel cell operation for practical use are currently under way, which would verify the importance of PES-PSA.

4. Conclusions

PES-PSA was synthesized by a coupling reaction using copper. The obtained polymer had an IEC of up to 1.58 meq/g and showed proton conductivity of up to 0.12 S/cm at 80 °C under 90% relative humidity. PES-PSA showed good fuel cell performance and high α -relaxation temperature and mechanical strength, which meant that PES-PSA can be one of the candidates as a mechanically tough membrane for fuel cells.

Acknowledgment. We thank the Sumika Chemical Analysis Services, Ltd. and the High Energy Accelerator Research Organization (K.E.K.) for help in the measurement of elemental analysis and SAXS, respectively.

Supporting Information Available: Text giving detailed experimental procedures and characterization of PES-PSA and SPES. This material is available free of charge via the Internet at <http://pubs.acs.org>.

References and Notes

- (1) Osborn, S. J.; Hassan, M. K.; Divoux, G. M.; Rhoades, D. W.; Mauritz, K. A.; Moore, R. B. *Macromolecules* **2007**, *40*, 3006–3890.
- (2) Hickner, M. A.; Ghassemi, H.; Kim, Y. S.; Einsla, B. R.; McGrath, J. E. *Chem. Rev.* **2004**, *104*, 4587–4612.
- (3) Rusanov, A. L.; Likhatchev, D.; Kostoglodov, P. V.; Mullen, K.; Klapper, M. *Adv. Polym. Sci.* **2005**, *179*, 83–134.
- (4) Li, Y.; Wang, F.; Yang, J.; Liu, D.; Roy, A.; Case, S.; Lesko, J.; McGrath, J. E. *Polymer* **2006**, *47*, 4210–4217.
- (5) Harrison, W. L.; Hickner, M. A.; Kim, Y. S.; McGrath, J. E. *Fuel Cell* **2005**, *2*, 201–212.
- (6) Ghassemi, H.; McGrath, J. E.; Zawodzinski, T. A. *Polymer* **2006**, *47*, 4132–4139.
- (7) Miyatake, K.; Chikashige, Y.; Watanabe, M. *Macromolecules* **2003**, *36*, 9691–9693.
- (8) Bailly, C.; Williams, D. J.; Karasz, F. E.; MacKnight, W. J. *Polymer* **1987**, *28*, 1009–1016.
- (9) Schmeller, E.; Ritter, H.; Ledjeff, K.; Nolte, R.; Thorwirth, R. Eur. Pat. 0574791 A2, **1993**.
- (10) Watari, T.; Fang, J.; Tanaka, K.; Kita, H.; Okamoto, K.; Hirano, T. *J. Membr. Sci.* **2004**, *230*, 111–120.
- (11) Fang, J.; Guo, X.; Harada, S.; Watari, T.; Tanaka, K.; Kita, H.; Okamoto, K. *Macromolecules* **2002**, *35*, 9022–9028.
- (12) Asano, N.; Miyatake, K.; Watanabe, M. *Chem. Mater.* **2004**, *16*, 2841–2843.
- (13) Guo, X.; Fang, J.; Watari, T.; Tanaka, K.; Kita, H.; Okamoto, K. *Macromolecules* **2002**, *35*, 6707–6713.
- (14) Miyatake, K.; Zhou, H.; Matsuo, T.; Uchida, H.; Watanabe, M. *Macromolecules* **2004**, *37*, 4961–4966.
- (15) Ghassemi, H.; McGrath, J. E. *Polymer* **2004**, *45*, 5847–5854.
- (16) Ghassemi, H.; Ndip, G.; McGrath, J. E. *Polymer* **2004**, *45*, 5855–5862.
- (17) Kobayashi, T.; Rikukawa, M.; Sanui, K.; Ogata, N. *Solid State Ionics* **1998**, *106*, 219–225.
- (18) Bae, J. M.; Honma, I.; Murata, M.; Yamamoto, T.; Rikukawa, M.; Ogata, N. *Solid State Ionics* **2002**, *147*, 189–194.
- (19) Koyama, T.; Kobayashi, T.; Yamaga, K.; Kamo, T.; Higashiyama, K. JP Patent 110174, **2002**.
- (20) Koyama, T.; Kobayashi, T.; Yamaga, K.; Kamo, T.; Higashiyama, K. U.S. Patent 0061431 A1, **2002**.
- (21) Zhou, H.; Miyatake, K.; Watanabe, M. *Fuel Cells* **2005**, *5*, 296–301.
- (22) Cho, C. G.; Kim, Y. S.; Yu, X.; Hill, M.; McGrath, J. E. *J. Polym. Sci., Part A: Polym. Chem.* **2006**, *44*, 6007–6014.
- (23) Mohr, R.; Kudela, V.; Schauer, J.; Richau, K. *Desalination* **2002**, *147*, 191–196.
- (24) Matsuo, S.; Muroya, S. JP Patent 186586, **1993**.
- (25) McLoughlin, V. C. R.; Thrower, J. U.S. Patent 3408411, **1968**.
- (26) McLoughlin, V. C. R.; Thrower, T. *Tetrahedron* **1969**, *25*, 5921–5940.
- (27) Kobayashi, Y.; Kumadaki, I. *Tetrahedron Lett.* **1969**, *47*, 4095–4096.
- (28) Mauritz, K. A.; Moore, R. B. *Chem. Rev.* **2004**, *104*, 4535–4585.
- (29) Hsu, W. Y.; Gierke, T. D. *J. Membr. Sci.* **1983**, *13*, 307–326.
- (30) Page, K. A.; Cable, K. M.; Moore, R. B. *Macromolecules* **2005**, *38*, 6472–6484.
- (31) Park, H. S.; Kim, Y. J.; Hong, W. H.; Lee, H. K. *J. Membr. Sci.* **2006**, *272*, 28–36.
- (32) Burgaz, E.; Lian, H.; Alonso, R. H.; Estevez, L.; Kelarakis, A.; Giannelis, E. P. *Polymer* **2009**, *50*, 2384–2392.
- (33) Mohamed, H. F. M.; Kobayashi, Y.; Kuroda, C. S.; Ohira, A. *J. Phys. Chem. B* **2009**, *113*, 2247–2252.
- (34) Stefanithis, I. D.; Mauritz, K. A. *Macromolecules* **1990**, *23*, 2397–2402.